Identification of a cuproptosis-related prognostic biomarker and therapeutic target in ovarian cancer

BINGXIN CHEN[1,2], SHUO YUAN[2] and HUI WANG[1,2]

[1]Department of Gynecologic Oncology, Women's Hospital, Zhejiang University School of Medicine, Hangzhou, Zhejiang 310006, P.R. China; [2]Zhejiang Provincial Key Laboratory of Precision Diagnosis and Therapy for Major Gynecological Diseases, Women's Hospital, Zhejiang University School of Medicine, Hangzhou, Zhejiang 310006, P.R. China

Received October 7, 2024; Accepted February 25, 2025

DOI: 10.3892/ol.2025.15048

Abstract. Ovarian cancer (OV) constitutes a significant hazard to the health of women and has low survival and high recurrence rates. Cuproptosis is a newly reported form of copper-dependent regulatory cell death. The present study identified cuproptosis-related long non-coding (lnc)RNAs in OV, highlighting their potential application as prognostic biomarkers and therapeutic targets. The RNA-sequencing data and clinical records of patients with OV were sourced from The Cancer Genome Atlas. Cuproptosis-related lncRNAs were filtered for their prognostic value using univariate and multivariate Cox regression, and least absolute shrinkage selection operator regression. Then, a risk model was formulated using these cuproptosis-related lncRNAs based on correlation coefficients. The risk model was calculated using the following formula: Risk = (0.687927022 x RP11-552D4.1) - (0.659783022 x AP001372.2) - (0.652465319 x RP11-505K9.1) - (1.627006889 x LINC00996). The predictive potential and clinical values of this risk model were identified through survival status, Kaplan-Meier survival curves, immune function, receiver operating characteristic curves, calibration curves, C-index and principal component analysis. Subsequently, the effects of LINC00996 (the lncRNA with the highest correlation coefficient in the risk model) on proliferation, metastasis and sensitivity to cuproptosis were assessed in OV cells. Finally, intracellular location of LINC00996 and the relative regulatory mechanism were predicted. In conclusion, the present study constructed a prognostic risk model based on lncRNAs associated with cuproptosis in OV, which can stratify risk and predict prognosis, and explored the regulatory mechanism of LINC00996 in cuproptosis.

Correspondence to: Professor Hui Wang, Department of Gynecologic Oncology, Women's Hospital, Zhejiang University School of Medicine, 1 Xueshi Road, Hangzhou, Zhejiang 310006, P.R. China
E-mail: wang71hui@zju.edu.cn

Key words: cuproptosis, long non-coding RNAs, risk model, ovarian cancer, RNA binding protein, microRNA

Introduction

Among gynecological malignancies, ovarian cancer (OV) exhibits the highest mortality rate and constitutes a significant hazard to the health of female patients (1). Specifically, there were 21,750 new OV cases and 13,940 deaths from OV in the United States in 2020 (2), and there were 57,090 new cases of OV and 39,306 deaths from OV in China in 2022 (3). Due to its deep pelvic location, lack of typical symptoms and lack of early screening tools, approximately two-thirds of patients have progressed to the advanced stage of disease at diagnosis, increasing the difficulty of treatment (4,5). Patients with stage I/II OV have a 10-year survival rate of 29-75%, whereas the 10-year survival rate drops to 6.9-22% for those with stage III-IV OV (6). Furthermore, >70% of patients with OV relapse within 2-3 years (7,8).

At present, the treatment of OV is multidisciplinary and comprehensive, which includes surgery, chemotherapy, targeted therapy and other therapeutic methods (5,9). However, the clinical effectiveness of these treatments is often compromised by drug resistance, cancer recurrence and immune escape (4,9). Consequently, there is an urgent need to identify novel molecular targets to improve the assessment of the progression of OV and enhance the available therapies.

Long non-coding (lnc)RNA refers to a category of RNA molecules whose transcript length is >200 nt (10). Due to the lack of conservative open reading frames, most lncRNAs are incapable of direct translation into proteins (11-13). However, lncRNA can recruit chromatin-remodeling complexes to regulate chromosome structure and modification (for instance, DNA methylation and histone modification), thus affecting gene expression levels (14,15). Chen and An (16) reported that the expression of lncRNA activated by TGF-β (ATB) is elevated in OV tissues compared with adjacent normal tissues, and it is linked to unfavorable outcomes. Furthermore, ATB facilitated the proliferation, invasion and migration of OV cells by mediating histone H3 lysine 27 trimethylation through binding to enhancer of zeste homolog 2 (16). lncRNAs also possess the capacity to regulate the transcription of target genes through interacting with transcriptional regulatory molecules (17-19). Moreover, lncRNA can bind RNA binding protein (RBP) to participate in alternative splicing, mRNA metabolism and transport (17,18,20). Gordon *et al* (21)

reported that high metastasis associated lung adenocarcinoma transcript 1 (MALAT1) expression is associated with increased stage, recurrence and decreased survival in OV, and that MALAT1 promotes OV progression by promoting the expression of RNA binding fox-1 homolog 2 and inhibiting preferential splicing of the pro-apoptotic isoform of kinesin family member 1b. Furthermore, lncRNA can function as a micro (mi)RNA sponge that reduces the activity of miRNA, thus enhancing the expression level of target genes (22). Zhou *et al* (23) reported that the expression levels of lncRNA isocitrate dehydrogenase 1 antisense RNA 1 (IDH1-AS1) are lower in epithelial OV cells than in normal ovarian epithelial cells, and IDH1-AS1 expression indicates a favorable prognosis. Additionally, IDH1-AS1 serves as a sponge for miR-518c-5p to suppress the proliferation of epithelial OV cells by targeting RNA binding motif protein 47 (23). In conclusion, lncRNAs serve a vital role in the progression of malignant tumors.

Regulated cell death (RCD) is a mode of cell death based on precise signaling networks and molecular mechanisms, and includes apoptosis, pyroptosis, necroptosis and ferroptosis (24,25). Recently, Tsvetkov *et al* (26) reported a new copper-dependent RCD, termed cuproptosis. Excess intracellular copper can interact with lipid-acylated proteins, which triggers irregular clustering of lipid-acylated proteins and depletion of iron-sulfur (Fe-S) clusters, ultimately culminating in cuproptosis (26). In addition, elesclomol (a potent copper ionophore) combined with copper can induce cuproptosis, whilst tetrathiopolybdate (a copper chelator) can inhibit cuproptosis, and cells with higher acylated protein level are more sensitive to cuproptosis (26). Ferrodoxin 1 functions as a vital positive regulator in cuproptosis, and other genes have also been identified as being closely related to cuproptosis (26-29). For instance, NLR family pyrin domain containing 3 (NLRP3) can be activated by intracellular copper, which can lead to cell death, whilst tetrathiopolybdate can inhibit NLRP3 activation (27). Furthermore, certain studies have reported that certain lncRNAs can regulate cuproptosis-related genes and are thereby considered novel potential targets in cuproptosis (30-33). For instance, LINC00996 has been identified as the key cuproptosis-related lncRNA in lung and bladder cancer (32,33). An in-depth study of cuproptosis could provide the ideal risk model and an accurate biomarker for malignant tumors; however, the function and underlying regulatory pathways of cuproptosis in OV are still poorly studied.

Therefore, the present study aimed to construct a prognostic risk model based on lncRNAs associated with cuproptosis in OV and to explore the regulatory mechanism of LINC00996 in cuproptosis in OV.

Materials and methods

Data collection and processing. The present study accessed the RNA sequencing (RNA-seq) data and clinical records of patients with OV from The Cancer Genome Atlas (TCGA)-OV dataset (https://portal.gdc.cancer.gov). The RNA-seq data was in fragments per Kilobase per Million format. The clinical records obtained included the age, stage, grade, survival status and survival time of the patients. A total of 378 patients with OV with complete data were randomly allocated to two groups, a training set (n=189) and a validation set (n=189), based on 'createDataPartition' package (rdocumentation.org/packages/caret/versions/6.0-94/topics/createDataPartition) in R programming (version 4.1.1). 'createDataPartition' uses the following basic syntax: createDataPartition (y, p=0.5, list=FALSE, …), with y representing the vector of outcomes and prepresenting percentage of data to use in the training set. The remaining data formed the validation set.

Identification of cuproptosis-related lncRNAs. Using the keywords 'cuproptosis,' 'copper' and 'regulated cell death' to search the PubMed (https://pubmed.ncbi.nlm.nih.gov/) and Web of Science (webofscience.com/) databases, articles related to cuproptosis were screened. Subsequently, by carefully reading the relevant articles, the cuproptosis-related genes and their functions were summarized. In addition, relevant reviews were consulted to identify other cuproptosis-related genes and their functions. Finally, 15 cuproptosis-related genes were obtained from previous studies (26-29). ENSEMBL (Release 111) (ensembl.org) was used to extract lncRNAs from the RNA-seq data. Subsequently, using the 'limma' packages (version 3.48.3) in R programming (version 4.1.1) and the Wilcoxon rank sum test, the Pearson correlation coefficients between lncRNA and cuproptosis-related genes were calculated. .The cut-off criteria included correlation coefficient (r) of >0.4 or <-0.4) and P<0.001. Additional notes that correlation coefficient |r| <0.4 indicated a weak correlation, 0.4 ~ 0.7 indicated a moderate correlation, and >0.7 indicated a strong correlation. Finally, a Sankey diagram was drawn based on the 'dplyr (version 1.0.7)', 'ggplot2 (version 3.4.0)' and 'ggalluvial (version 0.12.3)' packages in R programming (version 4.1.1).

Construction of the risk model. There was no discernible difference in the clinical characteristics between the training and the validation sets. Univariate Cox regression was performed to identify cuproptosis-related lncRNAs associated with overall survival (OS) in the training set. Among these lncRNAs, the risk model was constructed using least absolute shrinkage selection operator (LASSO) regression analysis and multivariate Cox regression. The risk score was calculated as follows: Risk score = $\sum^{n}_{k=1}$ coef(lncRNA^{k}) x expr(lncRNA^{k}), where coef(lncRNA) represents the link between the lncRNA and the survival of the patient with OV, and expr(lncRNA) represents the expression level of the lncRNA. The analysis was performed using R programming (version 4.1.1).

Identification of the prognostic signature. Patients with a risk score >1 were considered high-risk, while those with a risk score ≤1 were considered low-risk, and the survival status and immune function in the low- and high-risk groups were analyzed. Univariate and multivariate Cox regression analysis were performed to identify independent predictors. Kaplan-Meier survival curves were then produced to compare the difference in the survival rate between the low- and high-risk groups using the 'survival (version 3.4.0)' and 'survminer (version 0.4.9)' packages. Furthermore, receiver operating characteristic (ROC) curves, calibration curves, C-index and principal component analysis (PCA) were performed. The analysis was carried out by R programming (version 4.1.1).

Cell culture. OVCAR3 cells were acquired from the American Type Culture Collection and cultured in Roswell Park Memorial Institute-1640 medium with 10% fetal bovine serum (FBS; both Gibco, Thermo Fisher Scientific Corporation). The cells were incubated in an environment that mimicked physiological conditions, with an atmosphere containing 5% CO_2 to maintain an optimal pH level and ensure proper gas exchange, while being maintained at a constant temperature of 37˚C.

Transfection of small interference (si)RNA. The LINC00996 siRNA (siLINC00996) and control siRNA (siControl) were purchased from Shanghai GenePharma Co., Ltd. When the cell density reached 60-75%, the transfection solution was configured as follows: Solution A, 250 μl OPTI-MEM (Gibco, Thermo Fisher Scientific, Inc.) with 5 μl Lipo3000 (Invitrogen; Thermo Fisher Scientific Corporation); and solution B, 250 μl OPTI-MEM with 50 nM siRNA (Genepharma Corporation), which were both incubated at room temperature for 5 min. Subsequently, solutions A and B were mixed and incubated at room temperature for 20 min. Then, the medium was removed from a 6-well plate containing OVCAR3 cells, and 1500 μl serum-free medium and 500 μl mixed solution was added at room temperature. Finally, After incubation for 12 h, it was replaced with fresh medium and further cultured in an incubator with 5% CO2 at 37˚C for 48 h. The sequences of the siRNAs used were as follows: siLINC00996-1, 5'-GCUGUG UGAAAGGGUUUAATT-3' and 5'-UUAAACCCUUUCACA CAGCTT-3'; siLINC00996-2, 5'-CCGGCCUUAUUGUUU CUAUTT-3' and 5'-AUAGAAACAAUAAGGCCGGTT-3'; and siControl, 5'-UUCUCCGAACGUGUCACGUTT-3' and 5'-ACGUGACACGUUCGGAGAATT-3'.

Extraction of RNA and reverse transcription-quantitative polymerase chain reaction (RT-qPCR) analysis. Extraction of total RNA from OVCAR3 cells was performed using the RNA Extraction Kit (Vazyme Biotech Co., Ltd.) according to the manufacturer's protocol. RT was performed to convert RNA into cDNA with HiScript® II Q RT SuperMix (Vazyme Biotech Co., Ltd.) according to the manufacturer's protocol. RNA expression was measured by ChamQ Universal SYBR qPCR Master Mix (Vazyme Biotech Co., Ltd.) with ABI ViiA™ 7 real-time fluorescence quantitative PCR instrument equipped with ViiATM7 system. Thermocycling conditions are as follows: Pre-denaturation at 95˚C for 3 min, then 95˚C for 10 sec, 60˚C for 30 sec and 95˚C for 15 sec as 1 cycle for 40 cycles. The relative gene expression was calculated by $2^{-\Delta\Delta Cq}$ method with GAPDH as the control (34). The primers (Tsingke Corporation) used were as follows: LINC00996 forward, 5'-CTCTGCCACATCGTTCGGTTC-3' and reverse 5'-CTTCTTACGCTGCCAACTGCTAA-3'; and GAPDH forward, 5'-GGAGCGAGATCCCTCCAAAAT-3' and reverse, 5'-GGCTGTTGTCATACTTCTCATGG-3'.

Cell proliferation and migration assay. A Cell Counting Kit-8 (CCK-8) assay was performed to measure proliferative ability. OVCAR3 cells were cultured in a 96-well plate. After adding CCK-8 solution (Beyotime Institute of Biotechnology) for 1 h, the absorbance was measured at 490 nm based on microplate reader.

A Transwell assay was the performed to evaluate migration ability. A cell suspension including 2x10^5 cells without FBS was added to the upper chamber and medium with 20% FBS was added to the lower chamber of the Transwell plate. The cells were incubated at 37°C for 24 h. When the cells passed through the membrane, 4% paraformaldehyde and crystal violet were added to the upper chamber for 15 min at room temperature. The results were observed under an inverted optical microscope (Shanghai Optical Instrument Factory) and counted using ImageJ 1.8.0 software (National Institutes of Health).

Sensitivity to cuproptosis. Elesclomol can facilitate the transport of Cu^{2+} into cells. After entering the cells, Cu^{2+} directly binds to lipoylated enzymes and prompts the aggregation of lipoylated proteins and the dissipation of Fe-S cluster proteins, leading to proteotoxic stress and ultimately cuproptosis (26). Therefore, cuproptosis was induced by adding elesclomol-$CuCl_2$ (Medchemexpress Corporation; $1x10^{-9}$ M to 10^{-4} M into the medium of OVCAR3 cells in a 5% CO_2 incubator at 37°C for 4 h . CCK-8 solution (Beyotime Institute of Biotechnology) was added for 1 h to measure the number of living cells and thus assess the sensitivity of cells to cuproptosis, in which the absorbance was measured at 490 nm based on microplate reader.

Prediction of RBPs and target mRNA. The RBPs that can interact with LINC00996 were predicted using the ENCORI database (https://rnasysu.com/encori/). The filtering condition was CLIP Data ≥1 (results were supported by at least one cross-linking immunoprecipitation. Based on ENCORI, the target mRNAs of the aforementioned RBPs were predicted. Because of the large number of predicted target mRNAs, we set more stringent filtering criteria as follows: CLIP Data was ≥4 and the number of pan-cancer was ≥10, which meant the results were supported by ≥4 cross-linking immunoprecipitation and were validated in at least 10 cancer types. In addition, expression of target lncRNA in ovarian cancer patients was analyzed using the Gene Expression Profiling Interactive Analysis (GEPIA; gepia.cancer-pku.cn/), and locations of target lncRNA are predicted by lncLocator (csbio.sjtu.edu.cn/bioinf/lncLocator/).

Prediction of miRNA and target mRNA. The miRNAs that can interact with LINC00996 were identified using DIANA Tools (http://diana.imis.athena-innovation.gr/DianaTools/index.php). Furthermore, ENCORI was used to predict the target genes of the aforementioned miRNAs.

Statistical analysis. Statistical analyses were performed using R programming (version 4.1.1) (https://www.r-project.org/about.html) and GraphPad Prism 9 (version 9.0.0; Dotmatics). Statistical differences for three-group comparisons were determined using one-way ANOVA with Tukey's post hoc test. The CCK-8 assay data were analyzed two-way ANOVA with Tukey's post hoc test. All P-values were two-sided and $P<0.05$ was considered to indicate a statistically significant difference.

Results

Identification of cuproptosis-related lncRNAs with prognostic significance. The study flowchart is shown in Fig. 1. Based on previous articles and reviews related to

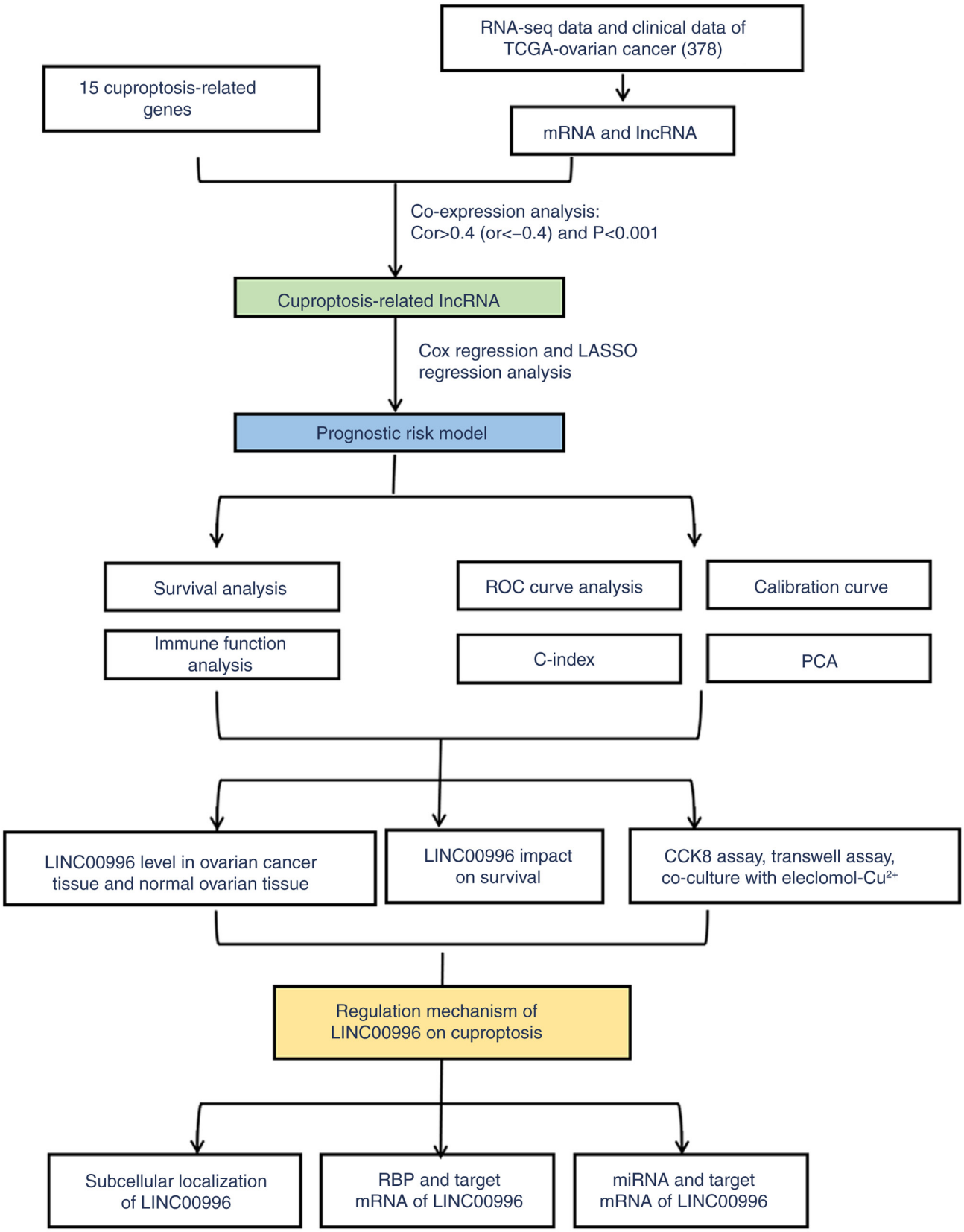

Figure 1. The research flowchart to construct the cuproptosis-related prognostic risk model in ovarian cancer. RNA-seq, RNA-sequencing; TCGA, The Cancer Genome Atlas; lncRNA, long non-coding RNA; LASSO, least absolute shrinkage selection operator; ROC, receiver operating characteristic; PCA, principal component analysis; CCK8, Cell Counting Kit 8; RBP, RNA binding protein; miRNA, microRNA.

cuproptosis, 15 cuproptosis-related genes were identified (Table SI) (26-29). Subsequently, 14,831 lncRNAs were obtained from TCGA-OV cohort through the ENSEMBL database. Pearson correlation analysis was performed to assess the correlation between cuproptosis-related genes and lncRNAs based on the 'limma (version 3.48.3)' packages

A

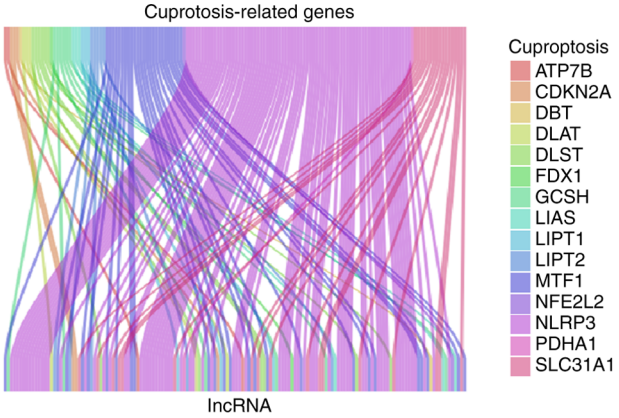

B

clinical features		whole group	training set	validation set	P-value
Age	<=65	259(68.52%)	128(67.72%)	131(69.31%)	0.8247
	>65	119(31.48%)	61(32.28%)	58(30.69%)	
Stage	Stage I-II	24(6.35%)	10(5.29%)	14(7.41%)	0.7113
	Stage III	294(77.78%)	151(79.89%)	143(75.66%)	
	Stage IV	57(15.08%)	27(14.29%)	30(15.87%)	
	unknown	3(0.79%)	1(0.53%)	2(1.06%)	
Grade	G1	1(0.26%)	0(0%)	1(0.53%)	0.568
	G2	45(11.9%)	24(12.7%)	21(11.11%)	
	G3	321(84.92%)	161(85.19%)	160(84.66%)	
	other	11(2.91%)	4(2.12%)	7(3.7%)	

C

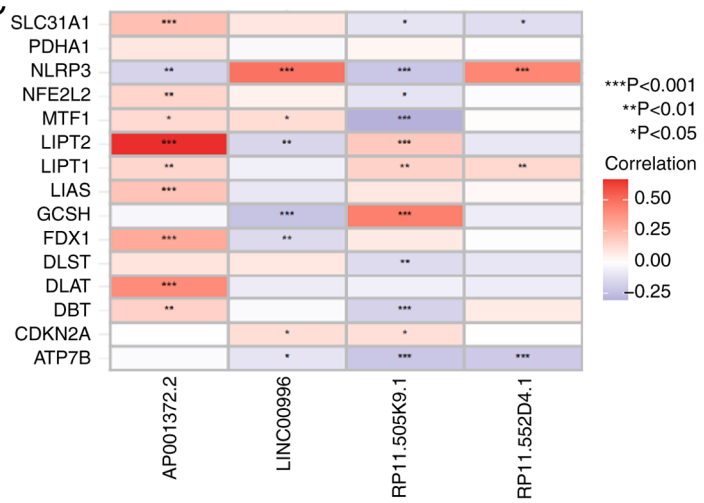

Figure 2. Identification of cuproptosis-related lncRNAs with prognostic significance in OV based on TCGA-OV cohort. (A) Sankey diagram was plotted according to the correlation between cuproptosis-related genes and lncRNAs. (B) Clinical characteristics of the training and validation sets based on TCGA-OV cohort. (C) Heat map of the correlations between 4 lncRNAs and genes associated with cuproptosis in the prognostic risk model. TCGA, The Cancer Genome Atlas; OV, ovarian cancer; lncRNA, long non-coding RNA.

and the Wilcoxon rank sum test. The criteria for cuproptosis-related lncRNAs were r>0.4 (or <-0.4) and P<0.001. Finally, 140 lncRNAs were identified as cuproptosis-related lncRNAs (Fig. 2A). The RNA-seq data and clinical records of 378 patients with OV were collected from TCGA-OV dataset. These patients with OV were randomly divided into a training set (n=189) and a validation set (n=189), both of which had similar clinical characteristics (Fig. 2B). Univariate Cox regression analysis was performed to identify the cuproptosis-related lncRNAs with prognostic significance in the training set. Among these lncRNAs, a risk model was constructed using LASSO regression and multivariate Cox regression. The risk model was calculated as the following formula: Risk = (0.687927022 x RP11-552D4.1) - (0.659783022 x AP001372.2) - (0.652465319 x RP11-505K9.1) - (1.627006889 x LINC00996). Among the lncRNAs identified, RP11-552D4.1 was found to be a risk factor, while AP001372.2, RP11-505K9.1 and LINC00996 were protective factors. The correlation between these 4 lncRNAs and the identified cuproptosis-related genes

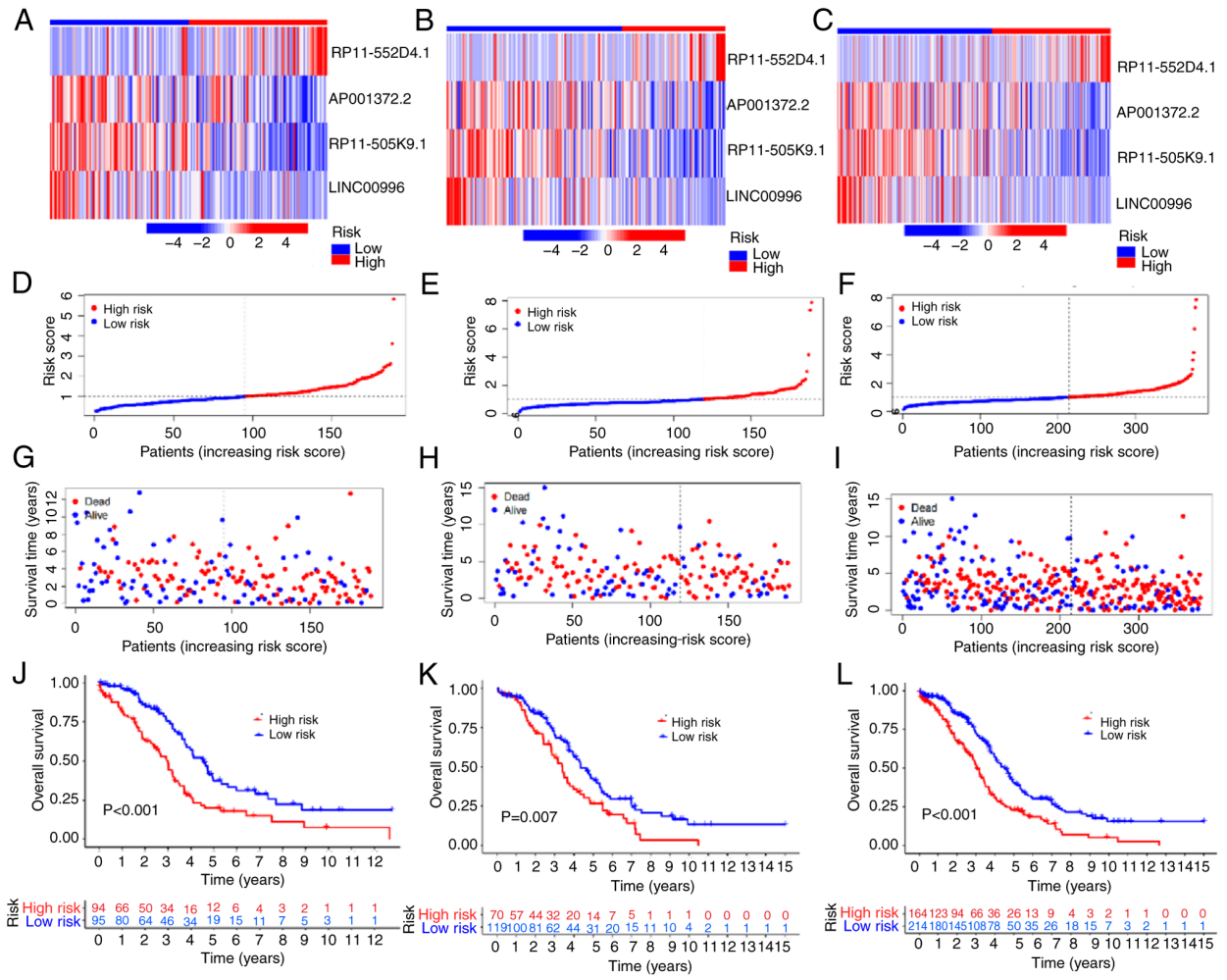

Figure 3. Predictive ability of the prognostic risk models. The expression levels of RP11-552D4.1, AP001372.2, RP11-505K9.1 and LINC00996 in the (A) training set, (B) validation set and (C) whole group. Patients in the (D) training set, (E) validation set and (F) whole group were divided into low-risk and high-risk groups. Survival status of the low-risk and high-risk groups in the (G) training set, (H) validation set and (I) whole group showed that compared with the low-risk group, more deaths were observed in the high-risk group. Kaplan-Meier survival curves of the low-risk and high-risk groups in the (J) training set, (K) validation set and (L) whole group showed that the prognosis for patients with ovarian cancer in the low-risk group was more superior. All the original data came from TCGA-OV cohort.

is shown in Fig. 2C. LINC00996 with the highest correlation coefficient in the risk model is significantly positively correlated with NLRP3 (P<0.001).

Predictive ability of the risk model. The expression of 4 lncRNAs (RP11.552D4.1, AP001372.2, RP11.505K9.1 and LINC00996) in the training set, validation set and whole group are shown using heat maps in Fig. 3A-C. Patients with a risk score of >1 were considered high-risk, while those with a risk score of ≤1 were considered low-risk. (Fig. 3D-F). Compared with the low-risk group, more deaths were observed in the high-risk group (Fig. 3G-I) in the training and validation set and whole group. Kaplan-Meier survival curves demonstrated that the prognosis of patients with OV in the low-risk group was superior compared with the high-risk group (training set, P<0.001; validation set, P=0.007; whole group, P<0.001; Fig. 3J-L). These results suggested that the risk model is reliable in predicting the prognosis of patients with OV.

Immune function analysis of the risk model. There is an association between cuproptosis and immune function (35). Excessive intracellular copper can lead to cuproptosis, which subsequently triggers immunogenic cell death and activates antitumor immune responses, thereby reprogramming the immunosuppressive tumor microenvironment (35,36). Moreover, cuproptosis-inducing drugs can markedly inhibit tumor growth and hold promising prospects for broad clinical application (35,36). Recent research has developed nanomedicines that can induce cuproptosis, which can notably inhibit tumor growth and promote immune responses, and in combination with programmed cell death 1 immunotherapy, they can markedly enhance antitumor efficacy (37). Thus, a thorough investigation into the association between cuproptosis and immune function holds promise for refining immunotherapy and enhancing antitumor efficacy in OV.

Based on immune function analysis, the generated heat map demonstrated that the high- and low-risk groups differed significantly in their immune functions (Fig. 4). The high-risk group had poorer immune functions in major histocompatibility complex (MHC)-class-I, type I interferon (IFN) response, chemokine receptor (CCR), antigen-presenting cell (APC) co-inhibition, parainflammation, human leukocyte

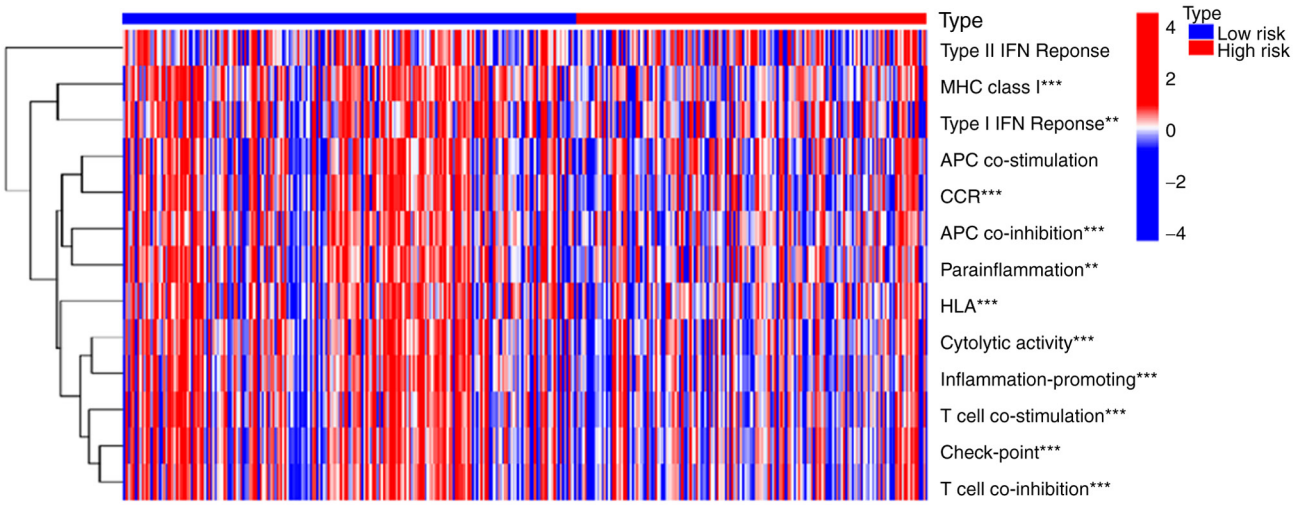

Figure 4. Immune function analysis of the risk model. The results showed that the high-risk group had poorer immune functions in MHC-class-I, type I IFN response, CCR, APC co-inhibition, parainflammation, HLA, cytolytic activity, inflammation-promoting, T cell co-stimulation, check-point and T cell co-inhibition. **P<0.01 and ***P<0.001. MHC, major histocompatibility complex; IFN, interferon; CCR, chemokine receptor; APC, antigen-presenting cell; HLA, human leukocyte antigen. All the original data came from TCGA-OV cohort.

antigen (HLA), cytolytic activity, inflammation-promoting, T cell co-stimulation, check-point and T cell co-inhibition. Therefore, the changes in immune function in the high-risk group may result in the progression of patients with OV.

Clinical significance of the risk model. Using univariate and multivariate Cox regression, the risk model was identified as an independent prognostic risk factor in OV (Fig. 5A and B). Additionally, the area under curve (AUC) of the ROC was calculated, which measured the prediction accuracy of the risk model. The closer the AUC value was to 1, the better the differentiation of the risk model and the higher the prediction accuracy of the risk model. As shown in Fig. 5C, the AUC of the risk model was 0.686, which demonstrated good differentiation and prediction accuracy. Moreover, the prognostic predictions of the risk model displayed good predictive performance for OS in patients with OV (1-year, AUC=0.686; 3-year, AUC=0.655; and 5-year, AUC=0.644; Fig. 5D). The calibration curve for 1-, 3- and 5-year OS also showed reliable predictive ability of the risk model (Fig. 5E) and the C-index of the risk model outranked that of other factors (Fig. 5F). Furthermore, PCA was performed based on all genes (Fig. 6A), the cuproptosis-related gene set (Fig. 6B), the cuproptosis-related lncRNA set (Fig. 6C) and the risk model (Fig. 6D). There were markedly different distribution of the high- and low-risk groups in the PCA based on the risk model, suggesting that the risk model may serve as a promising biomarker for risk stratification. In summary, the risk model could accurately predict prognosis and has notable clinical value.

Effect of LINC00996 in patients with OV. In the risk model, the correlation coefficient of LINC00996 was the highest compared with the other lncRNAs, indicating that it may serve a crucial role in cuproptosis in OV. Certain studies have reported the function of LINC00996 in several malignant tumors, such as colorectal cancer and lung adenocarcinoma, yet its potential role and importance in OV remain incompletely understood (38,39). Furthermore, data from GEPIA suggested that the LINC00996 expression level is lower in patients with OV with a higher International Federation of Gynecology and Obstetrics (FIGO) stage compared with those with a lower FIGO stage (40) (Fig. 7A). Kaplan-Meier survival curves also demonstrated that the lower the expression of LINC00996, the lower the survival rate of patients with OV (Fig. 7B). These results suggest that LINC00996 may serve an inhibitory role in OV.

Effect of LINC00996 on the biological behavior of OV cells. After transfecting siLINC00996-1 and siLINC00.996-2 into OVCAR3 cells to knockdown LINC00996 expression, the role of LINC00996 in OV cells was further explored (Fig. 8A). The results of the CCK-8 assay revealed that knockdown of LINC00996 improved the proliferative ability of OV cells (Fig. 8B). Moreover, the results of the Transwell assay demonstrated that the knockdown of LINC00996 enhanced the migration ability of OV cells (Fig. 8C and D). Elesclomol facilitates the intracellular translocation of Cu^{2+}, thereby inducing mitochondrial dysfunction and triggering cuproptosis (26). After culturing the cells with different concentrations of elesclomol-Cu^{2+} solution (ranging from 10^{-9} to 10^{-4} mol/l), a CCK-8 assay was performed to assess the sensitivity of the cells to cuproptosis. The results suggested that the knockdown of LINC00996 reduced the sensitivity of OV cells to cuproptosis (Fig. 8E).

Regulatory mechanism of LINC00996 binding to ELAV-like RNA binding protein 1 (ELAVL1) in cuproptosis. Based on the results from lncLocator, LINC00996 was determined to be primarily located in the cytoplasm (Fig. 9A). This subcellular localization suggested that LINC00996 may bind to RBPs or act as an miRNA sponge. According to the correlation between LINC00996 and genes associated with cuproptosis, LINC00996 was significantly positively correlated with NLRP3 (P<0.001) (Fig. 2C). Moreover, to predict the RBPs that can bind to LINC00996 as well as the target mRNAs, stringent filtering conditions were set in ENCORI. RBPs

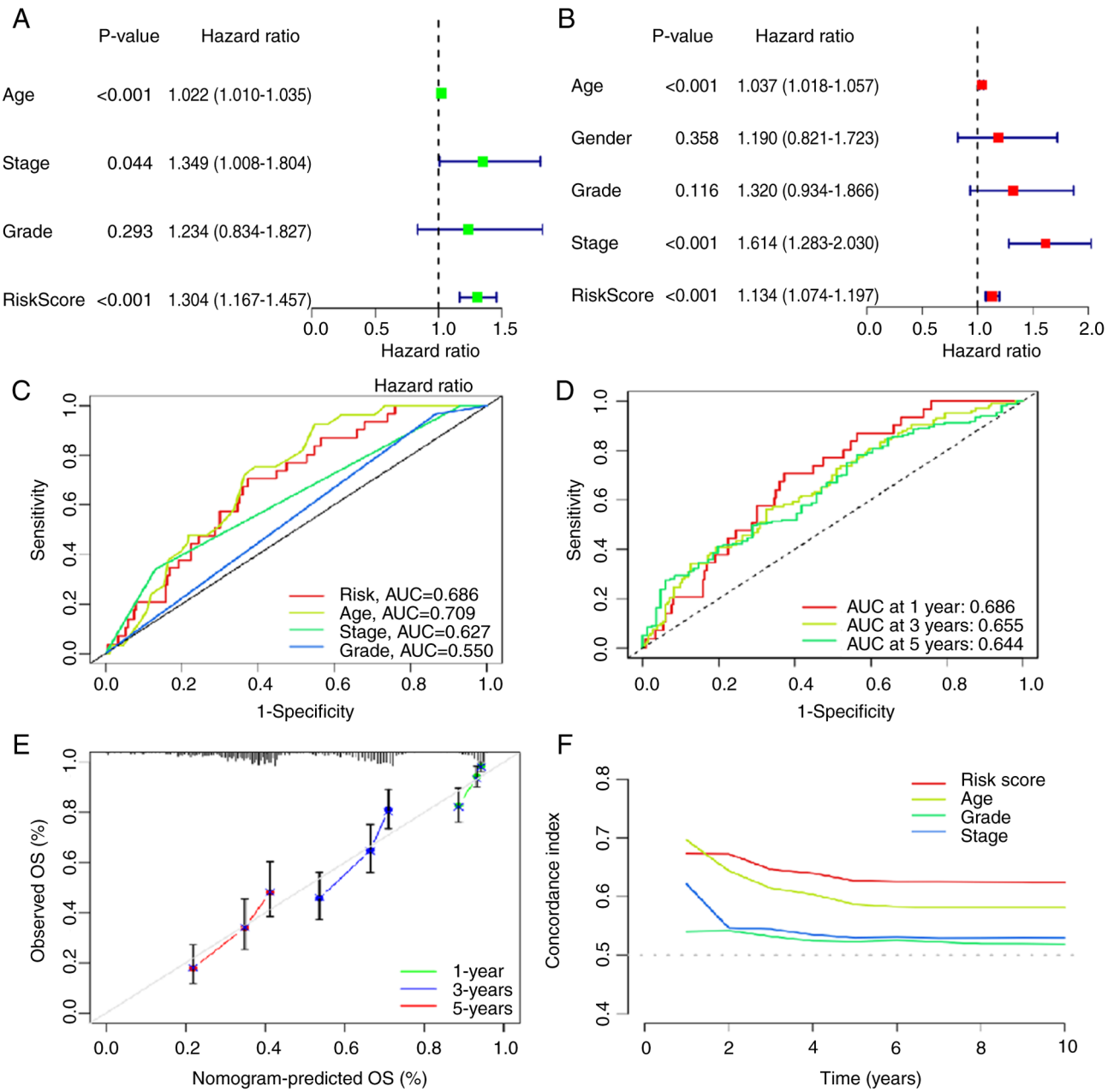

Figure 5. Clinical value of the risk model. (A) Univariate analysis and (B) multivariate analysis demonstrated that the risk model was an independent prognostic risk factor for patients with OV. (C) Receiver operating characteristic curve of the risk model displayed good differentiation and prediction accuracy. (D) AUC values of risk model displayed notable precision and accuracy in patients with OV. (E) The calibration curve for 1-, 3- and 5-year OS showed reliable predictive ability of the risk model. (F) Concordance index of the risk model outranked that of other factors. OV, ovarian cancer; AUC, area under the curve; OS, overall survival. All the original data came from TCGA-OV cohort, and the analysis was carried out by R.

interacting with LINC00996 were predicted using ENCORI, filtered by CLIP Data ≥1. The results showed that ELAVL1 and muscleblind-like splicing regulator 1 may bind to LINC00996. Subsequently, the target mRNAs of the aforementioned two RBPs were predicted, filtered by CLIP Data ≥4 and pan-cancer count ≥10. The results suggested that ELAVL1 could interact with NLRP3 mRNA (Fig. 9B).

Regulatory mechanism of LINC00996 as an miRNA sponge in cuproptosis. Previous studies have suggested that miRNA recognize and bind to target mRNA, typically promoting mRNA degradation or inhibiting its translation. Additionally, lncRNAs can bind to specific miRNAs and modulate the expression levels of the target mRNAs, thereby forming a regulatory network consisting of lncRNA-miRNA-mRNA (22). In the present study, the miRNAs that interact with LINC00996 were predicted utilizing the DIANA tools. The findings revealed that hsa-miR-20a-5p, hsa-miR-106a-5p, hsa-miR-106b-5p, hsa-miR-17-5p, hsa-miR-34a-5p and hsa-miR-93-5p could interact with LINC00996. Based on ENCORI, the target mRNAs of these 6 miRNAs were then predicted (Fig. 10A). Consequently, a comprehensive lncRNA-miRNA-mRNA regulatory network pertinent to cuproptosis was constructed (Fig. 10B). Notably, among the aforementioned 6 miRNAs, hsa-miR-106a-5p, hsa-miR-106b-5p, hsa-miR-17-5p and hsa-miR-93-5p may act on NLRP3 mRNA. This comprehensive

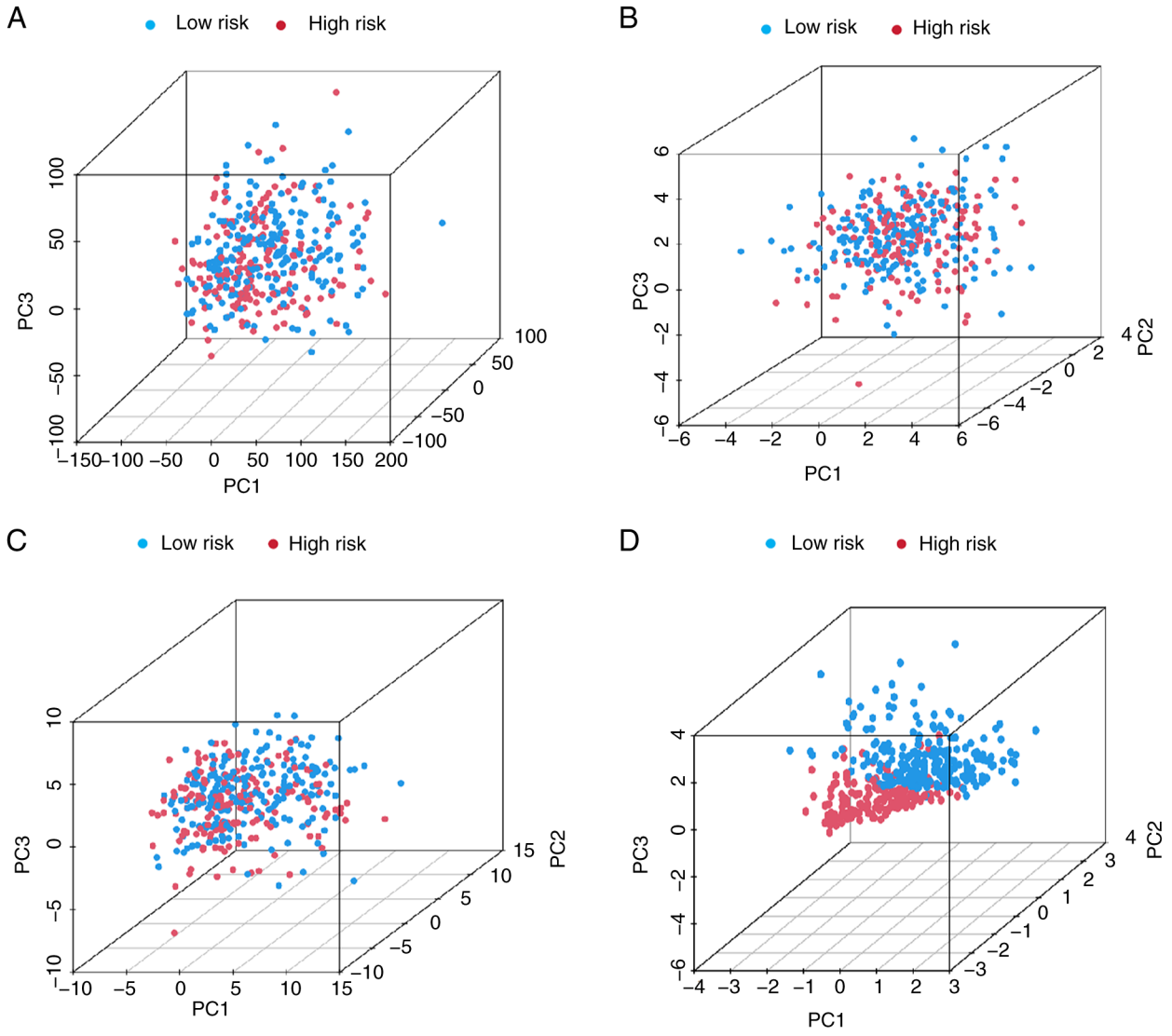

Figure 6. PCA of the risk model. The PCA based on (A) all genes, (B) the cuproptosis-related gene set, (C) the cuproptosis-related long non-coding RNA set and (D) the risk model. The results showed different distribution of the high-risk and low-risk groups in PCA based on the risk model. PCA, principal component analysis. All the original data came from TCGA-OV cohort, and the analysis was carried out by R programming (version 4.1.1).

lncRNA-miRNA-mRNA regulatory network will be further verified in subsequent studies.

Discussion

In the present study, after analyzing the TCGA-OV cohort, a prognostic risk model based on cuproptosis-associated lncRNAs was constructed. Survival analysis, ROC curves, calibration curves, C-index and PCA demonstrated the reliability of the constructed risk model. The potential mechanism of LINC00996 in the aforementioned risk model was then predicted using ENCORI and DIANA tools. The prognostic risk model can divide patients with OV into high- and low-risk groups. Furthermore, the immune function analysis demonstrated that MHC-class-I, type I IFN response, CCR, APC co-inhibition, parainflammation, HLA, cytolytic activity, inflammation-promoting, T cell co-stimulation, check-point and T cell co-inhibition were improved in the low-risk group (41-45). MHC-class-I can present intracellular peptides, which are recognized by $CD8^+$ T cells, thus inducing an antitumor immune response (41-43). The findings of the present study suggested that the low-risk group had a more optimal immune function in MHC-class-I, indicating that the improved prognosis in the low-risk group may be associated with the antitumor immune response induced by MHC-class-I. However, the effect of different immune functions between groups on the prognosis of patients with OV needs further analysis and experimental verification.

Excess intracellular copper can interact with lipid acylated proteins, and this process triggers irregular clustering of lipid-acylated proteins and depletion of Fe-S clusters, ultimately culminating in cuproptosis (26,46). However, the role of cuproptosis in tumor progression and its regulatory mechanism are poorly understood. The present study constructed a prognostic risk model of lncRNAs associated with cuproptosis and demonstrated that patients with OV in low-risk group had an improved prognosis. We hypothesized that patients with OV in the low-risk group would be more sensitive to cuproptosis than those in the high-risk group. Cuproptosis provides new perspectives on the treatment approach of OV, and the

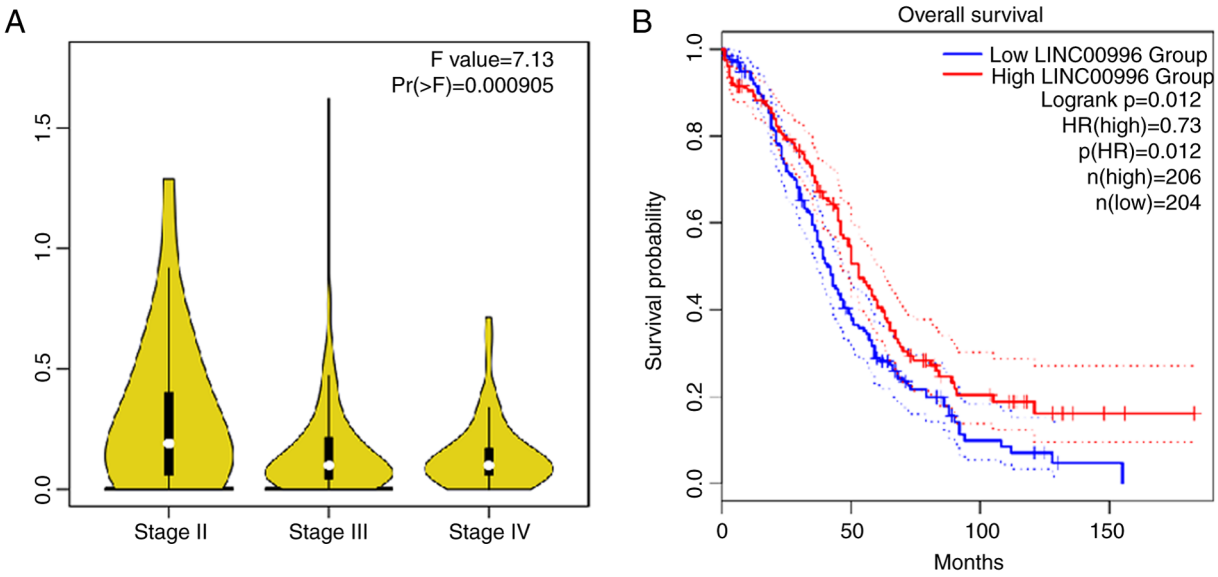

Figure 7. LINC00996 may play an antitumor role in OV. (A) The levels of LINC00996 in OV at different International Federation of Gynecology and Obstetrics stages according to GEPIA. (B) Kaplan-Meier survival curve showed that low expression of LINC00996 was associated with a lower the survival rate in patients with OV according to GEPIA. OV, ovarian cancer; HR, hazard ratio.

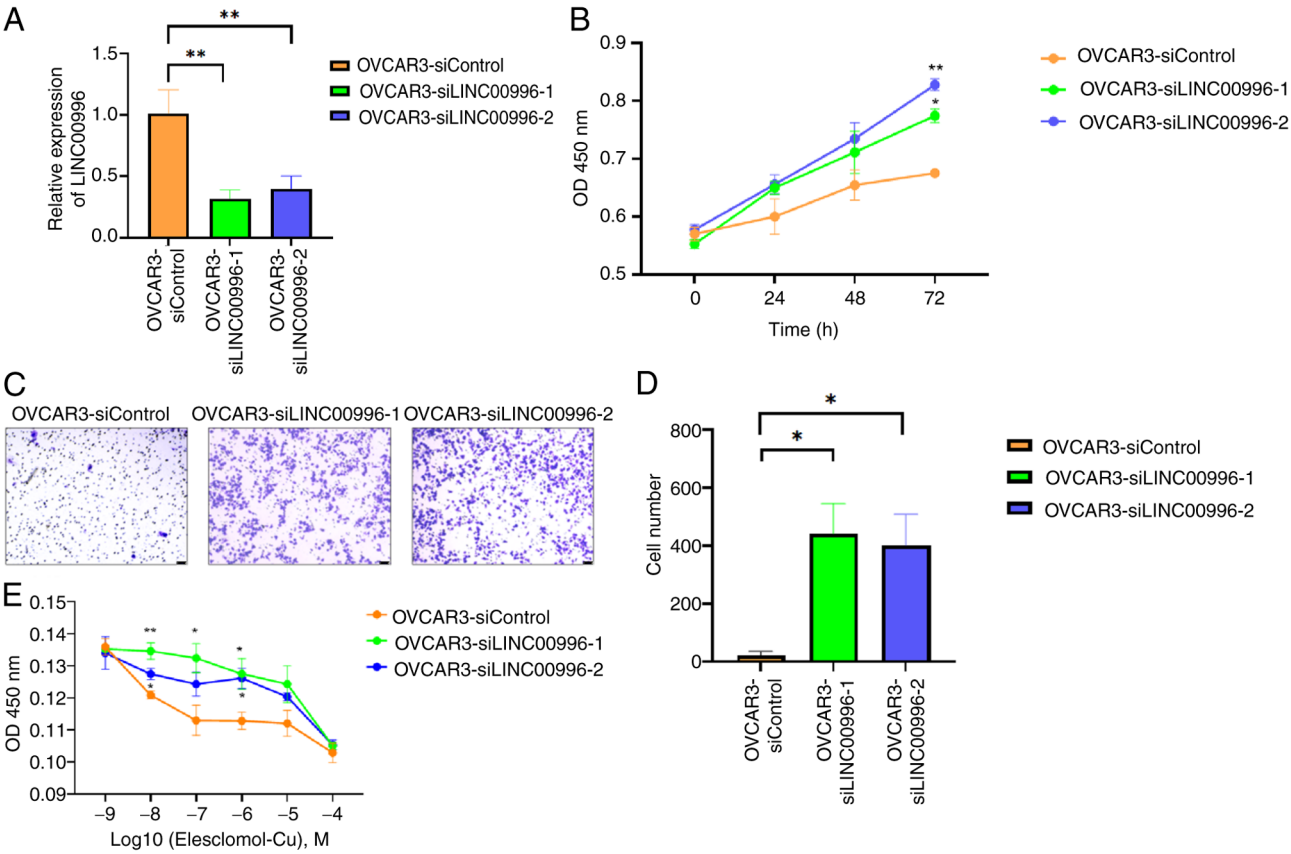

Figure 8. Effect of LINC00996 on the biological behavior of OVCAR3 cells. (A) LINC00996 was knocked down in OVCAR3 cells through transfection with siRNA. (B) CCK-8 assay demonstrated that knocking down LINC00996 can improve the proliferative ability of OVCAR3 cells. (C) Transwell assay of OVCAR3-siControl, -siLINC00996-1 and OVCAR3-siLINC00996-2 (scale bar, 50 μm). (D) Transwell assay demonstrated that knocking down LINC00996 can enhance the migration ability of OVCAR3 Cells. (E) CCK-8 assay demonstrated that knocking down LINC00996 can reduce the sensitivity of OVCAR3 Cells to cuproptosis. *P<0.05, **P<0.01 vs. siControl. si, small interfering RNA; CCK-8, Cell Counting Kit-8.

induction of cuproptosis may be an emerging treatment option. Moreover, O'Day *et al* (47) reported that combination therapy of elesclomol and paclitaxel could markedly increase the survival rate of patients with stage IV metastatic melanoma. In the present study, after culturing with elesclomol-Cu^{2+}, the sensitivity of OV cells to cuproptosis was positively associated

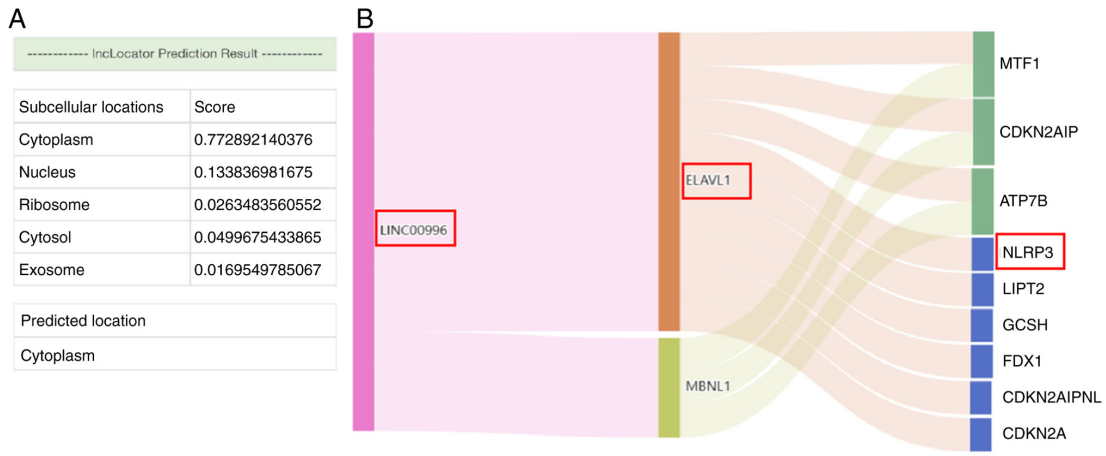

Figure 9. Mechanism of LINC00996 binding to ELAVL1 to regulate cuproptosis. (A) LINC00996 was mainly located in the cytoplasm according to lncLocator. (B) Prediction of the RNA binding proteins of LINC00996 and target RNAs according to the ENCORI. The results suggested that ELAVL1 could interact with NLRP3 mRNA. ELAVL1, ELAV-like RNA binding protein 1; NLRP3, NLR family pyrin domain containing 3.

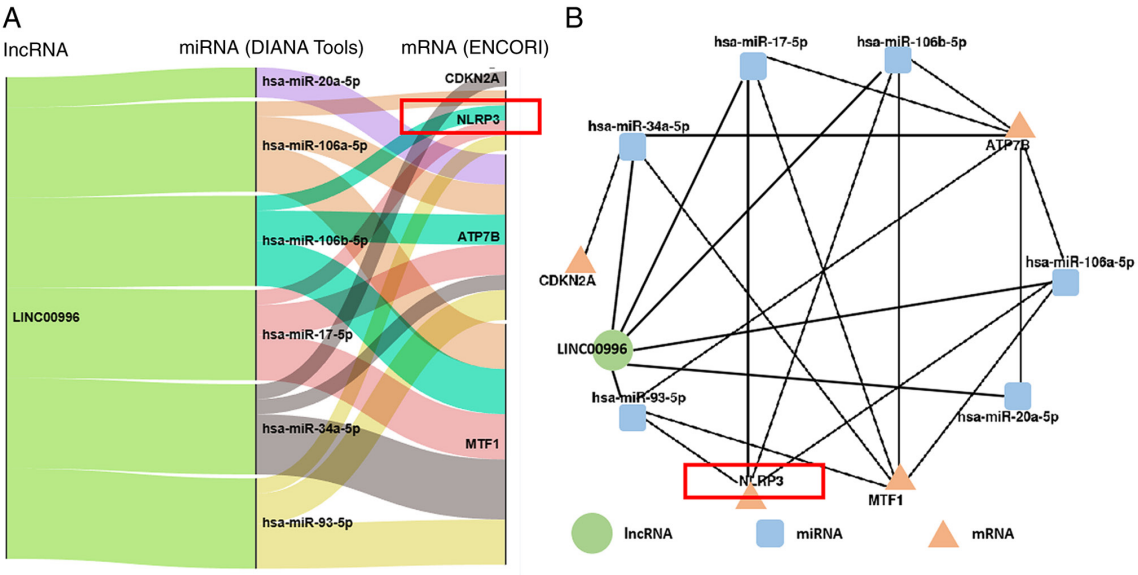

Figure 10. Mechanism of LINC00996 as a miRNA sponge to regulate cuproptosis. The DIANA tools was used to predict the miRNAs that interact with LINC00996, and ENCORI was used to predict the target genes of these miRNAs. hsa-miR-20a-5p, hsa-miR-106a-5p, hsa-miR-106b-5p, hsa-miR-17-5p, hsa-miR-34a-5p and hsa-miR-93-5p could interact with LINC00996. The target mRNAs of these 6 miRNAs were further predicted. The results were shown in (A) Sankey and (B) competing endogenous RNA network diagrams. miR, microRNA; lncRNA, long non-coding RNA.

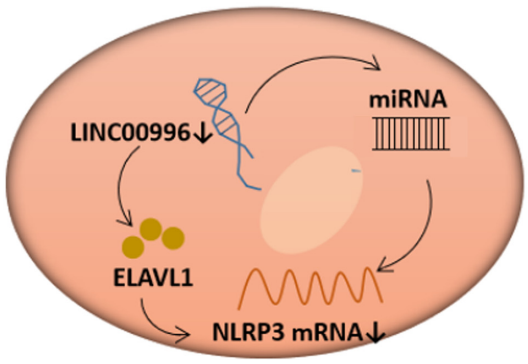

Figure 11. Schematic diagram. The reduction of LINC00996 in ovarian cancer can regulate NLRP3 mRNA by decreasing the binding of ELAVL1 or acting as an miRNA sponge, thereby reducing the sensitivity to cuproptosis. ELAVL1, ELAV-like RNA binding protein 1; NLRP3, NLR family pyrin domain containing 3; miRNA; microRNA.

with the level of LINC00996. Therefore, LINC00996 could be a new prognostic biomarker for OV, and the induction of cuproptosis may be a potent treatment for patients with OV.

The key lncRNA of the prognostic risk model in the present study was LINC00996, which was significantly positively correlated with the cuproptosis-related gene, NLRP3. According to previous reports, lncRNAs that are located in the nucleus can regulate chromatin structure and histone modifications and affect gene transcription, while lncRNAs that are localized in the cytoplasm can regulate mRNA translation and degradation (48,49). LINC00996 is mainly localized in the cytoplasm, suggesting that LINC00996 regulates cuproptosis in OV through binding RBPs or acting as an miRNA sponge (Fig. 11). Data from ENCORI suggested that the RBP, ELAVL1, can bind to LINC00996. ELAVL1 can increase mRNA stability and serves a vital role in tumor

progression (50,51). Additionally, NLRP3 was the target mRNA of ELAVL1 based on ENCORI. ELAVL1 can bind to adenine and uridine-rich stability elements to improve mRNA stability (52-55). Liu *et al* (56) reported that in rheumatoid arthritis fibroblast-like synoviocytes and human umbilical vein endothelial cells, the nucleocytoplasmic shuttling of ELAVL1 is initiated and ELAVL1 expression is notably elevated in the cytoplasm, which increases the stability of NLRP3 mRNA and promotes NLRP3 expression, after TNF-α and calreticulin dual stimulation. Furthermore, in high glucose-treated cardiomyocytes and in human diabetic hearts, Jeyabal *et al* (57) also reported that ELAVL1 knockdown reduced the expression level of NLRP3. Therefore, we hypothesized that LINC00996 can increase the stability of NLRP3 mRNA by binding to ELAVL1 in OV cells, thereby regulating sensitivity to cuproptosis. The present study found that LINC00996, as a sponge, can bind to hsa-miR-20a-5p, hsa-miR-106a-5p, hsa-miR-106b-5p, hsa-miR-17-5p, hsa-miR-34a-5p and hsa-miR-93-5p. Among these miRNA, hsa-miR-106a-5p, hsa-miR-106b-5p, hsa-miR-17-5p and hsa-miR-93-5p can act on NLRP3 mRNA.

The present study has the following limitations: First, it used a dataset of 378 patients with OV from TCGA to explore a cuproptosis-related risk model, but further validation of the risk model in cohorts from other institutions is needed to ensure broader applicability. Second, while preliminary validation was performed using cell experiments, further *in vitro* and *in vivo* experiments are required to verify the interactions and regulatory mechanisms.

In conclusion, the present study constructed a prognostic risk model based on lncRNAs associated with cuproptosis in OV and explored the regulatory mechanism of LINC00996 in cuproptosis. The results provide new perspectives to assess the role of cuproptosis in OV; however, more validation experiments are required to further explore this role.

Acknowledgements

Not applicable.

Funding

This study was funded by Natural Science Foundation of Zhejiang Province (grant no. LQ23H160033), Zhejiang Medical and Health Science and Technology program (grant no. 2024KY116) and Key R&D Program of Zhejiang Province (grant no. 2022C03013).

Availability of data and materials

The data generated in the present study may be requested from the corresponding author.

Authors' contributions

BC and HW proposed the conception and implementation of the study. BC and SY were responsible for data download and the interpretation of data. BC was a major contributor in the preparation of the manuscript. BC and HW performed the final proofreading. BC, SY and HW confirm the authenticity of all the raw data. All authors read and approved the final version of the manuscript.

Ethics approval and consent to participate

Not applicable.

Patient consent for publication

Not applicable.

Competing interests

The authors declare that they have no competing interests.

References

1. Siegel RL, Miller KD, Fuchs HE and Jemal A: Cancer statistics, 2022. CA Cancer J Clin 72: 7-33, 2022.
2. Siegel RL, Miller KD, Goding SA, Fedewa SA, Butterly LF, Anderson JC, Cercek A, Smith RA and Jemal A: Colorectal cancer statistics, 2020. CA Cancer J Clin 70: 145-164, 2020.
3. Xia C, Dong X, Li H, Cao M, Sun D, He S, Yang F, Yan X, Zhang S, Li N and Chen W: Cancer statistics in China and United States, 2022: Profiles, trends, and determinants. Chin Med J (Engl) 135: 584-590, 2022.
4. Chen S, Tang Y, Li Y, Huang M, Ma X, Wang L, Wu Y, Wang Y, Fan W and Hou S: Design and application of prodrug fluorescent probes for the detection of ovarian cancer cells and release of anticancer drug. Biosens Bioelectron 236: 115401, 2023.
5. Li T, Wang X, Qin S, Chen B, Yi M and Zhou J: Targeting PARP for the optimal immunotherapy efficiency in gynecologic malignancies. Biomed Pharmacother 162: 114712, 2023.
6. Kahn R, Filippova O, Gordhandas S, An A, Straubhar AM, Zivanovic O, Gardner GJ, O'Cearbhaill RE, Tew WP, Grisham RN, *et al*: Ten-year conditional probability of survival for patients with ovarian cancer: A new metric tailored to long-term survivors. Gynecol Oncol 169: 85-90, 2023.
7. Singh N, Jayraj AS, Sarkar A, Mohan T, Shukla A and Ghatage P: Pharmacotherapeutic treatment options for recurrent epithelial ovarian cancer. Expert Opin Pharmacother 24: 49-64, 2023.
8. Perren TJ, Swart AM, Pfisterer J, Ledermann JA, Pujade-Lauraine E, Kristensen G, Carey MS, Beale P, Cervantes A, Kurzeder C, *et al*: A phase 3 trial of bevacizumab in ovarian cancer. N Engl J Med 365: 2484-2496, 2011.
9. Bi R, Chen L, Huang M, Qiao Z, Li Z, Fan G and Wang Y: Emerging strategies to overcome PARP inhibitors' resistance in ovarian cancer. Biochim Biophys Acta Rev Cancer 1879: 189221, 2024.
10. Ponting CP, Oliver PL and Reik W: Evolution and functions of long noncoding RNAs. Cell 136: 629-641, 2009.
11. Zhao J, Sun J, Shuai SC, Zhao Q and Shuai J: Predicting potential interactions between lncRNAs and proteins via combined graph auto-encoder methods. Brief Bioinform 24: bbac527, 2023.
12. Tang Y, Cheung BB, Atmadibrata B, Marshall GM, Dinger ME, Liu PY and Liu T: The regulatory role of long noncoding RNAs in cancer. Cancer Lett 391: 12-19, 2017.
13. Yao ZT, Yang YM, Sun MM, He Y, Liao L, Chen KS and Li B: New insights into the interplay between long non-coding RNAs and RNA-binding proteins in cancer. Cancer Commun (Lond) 42: 117-140, 2022.
14. Zhou HL, Luo G, Wise JA and Lou H: Regulation of alternative splicing by local histone modifications: Potential roles for RNA-guided mechanisms. Nucleic Acids Res 42: 701-713, 2014.
15. Gupta RA, Shah N, Wang KC, Kim J, Horlings HM, Wong DJ, Tsai MC, Hung T, Argani P, Rinn JL, *et al*: Long non-coding RNA HOTAIR reprograms chromatin state to promote cancer metastasis. Nature 464: 1071-1076, 2010.
16. Chen XJ and An N: Long noncoding RNA ATB promotes ovarian cancer tumorigenesis by mediating histone H3 lysine 27 trimethylation through binding to EZH2. J Cell Mol Med 25: 37-46, 2021.
17. Statello L, Guo CJ, Chen LL and Huarte M: Gene regulation by long non-coding RNAs and its biological functions. Nat Rev Mol Cell Biol 22: 96-118, 2021.

18. Quinn JJ and Chang HY: Unique features of long non-coding RNA biogenesis and function. Nat Rev Genet 17: 47-62, 2016.
19. Liu SS, Li JS, Xue M, Wu WJ, Li X and Chen W: LncRNA UCA1 participates in De Novo synthesis of guanine nucleotides in bladder cancer by recruiting TWIST1 to increase IMPDH1/2. Int J Biol Sci 19: 2599-2612, 2023.
20. Haas R, Ganem NS, Keshet A, Orlov A, Fishman A and Lamm AT: A-to-I RNA editing affects lncRNAs expression after heat shock. Genes (Basel) 9: 627, 2018.
21. Gordon MA, Babbs B, Cochrane DR, Bitler BG and Richer JK: The long non-coding RNA MALAT1 promotes ovarian cancer progression by regulating RBFOX2-mediated alternative splicing. Mol Carcinog 58: 196-205, 2019.
22. Ma B, Wang S, Wu W, Shan P, Chen Y, Meng J, Xing L, Yun J, Hao L, Wang X, *et al*: Mechanisms of circRNA/lncRNA-miRNA interactions and applications in disease and drug research. Biomed Pharmacother 162: 114672, 2023.
23. Zhou J, Xu Y, Wang L, Cong Y, Huang K, Pan X, Liu G, Li W, Dai C, Xu P and Jia X: LncRNA IDH1-AS1 sponges miR-518c-5p to suppress proliferation of epithelial ovarian cancer cell by targeting RMB47. J Biomed Res 38: 51-65, 2023.
24. Kalkavan H, Rühl S, Shaw JJP and Green DR: Non-lethal outcomes of engaging regulated cell death pathways in cancer. Nat Cancer 6: 795-806, 2023.
25. Tong X, Tang R, Xiao M, Xu J, Wang W, Zhang B, Liu J, Yu X and Shi S: Targeting cell death pathways for cancer therapy: Recent developments in necroptosis, pyroptosis, ferroptosis, and cuproptosis research. J Hematol Oncol 15: 174, 2022.
26. Tsvetkov P, Coy S, Petrova B, Dreishpoon M, Verma A, Abdusamad M, Rossen J, Joesch-Cohen L, Humeidi R, Spangler RD, *et al*: Copper induces cell death by targeting lipoylated TCA cycle proteins. Science 375: 1254-1261, 2022.
27. Deigendesch N, Zychlinsky A and Meissner F: Copper regulates the canonical NLRP3 inflammasome. J Immunol 200: 1607-1617, 2018.
28. Xue Q, Kang R, Klionsky DJ, Tang D, Liu J and Chen X: Copper metabolism in cell death and autophagy. Autophagy 19: 2175-2195, 2023.
29. Liu S, Ge J, Chu Y, Cai S, Wu J, Gong A and Zhang J: Identification of hub cuproptosis related genes and immune cell infiltration characteristics in periodontitis. Front Immunol 14: 1164667, 2023.
30. Sun M, Zhan N, Yang Z, Zhang X, Zhang J, Peng L, Luo Y, Lin L, Lou Y, You D, *et al*: Cuproptosis-related lncRNA JPX regulates malignant cell behavior and epithelial-immune interaction in head and neck squamous cell carcinoma via miR-193b-3p/PLAU axis. Int J Oral Sci 16: 63, 2024.
31. Zhou G, Chen C, Wu H, Lin J, Liu H, Tao Y and Huang B: LncRNA AP000842.3 triggers the malignant progression of prostate cancer by regulating cuproptosis related gene NFAT5. Technol Cancer Res Treat 23: 15330338241255585, 2024.
32. Bai Y, Zhang Q, Liu F and Quan J: A novel cuproptosis-related lncRNA signature predicts the prognosis and immune landscape in bladder cancer. Front Immunol 13: 1027449, 2022.
33. Huang H, Chen G, Zhang Z, Wu G, Zhang Z, Yu A, Wang J, Quan C, Li Y and Zhou M: Deciphering the role of cuproptosis-related lncRNAs in shaping the lung cancer immune microenvironment: A comprehensive prognostic model. J Cell Mol Med 28: e18519, 2024.
34. Livak KJ and Schmittgen TD: Analysis of relative gene expression data using real-time quantitative PCR and the 2(-Delta Delta C(T)) method. Methods 25: 402-408, 2001.
35. Wu H, Lu X, Hu Y, Baatarbolat J, Zhang Z, Liang Y, Zhang Y, Liu Y, Lv H and Jin X: Biomimic nanodrugs overcome tumor immunosuppressive microenvironment to enhance cuproptosis/chemodynamic-induced cancer immunotherapy. Adv Sci (Weinh) 12: e2411122, 2025.
36. Guan M, Cheng K, Xie XT, Li Y, Ma MW, Zhang B, Chen S, Chen W, Liu B, Fan JX and Zhao YD: Regulating copper homeostasis of tumor cells to promote cuproptosis for enhancing breast cancer immunotherapy. Nat Commun 15: 10060, 2024.
37. Lu X, Chen X, Lin C, Yi Y, Zhao S, Zhu B, Deng W, Wang X, Xie Z, Rao S, *et al*: Elesclomol loaded copper oxide nanoplatform triggers cuproptosis to enhance antitumor immunotherapy. Adv Sci (Weinh) 11: e2309984, 2024.
38. Shen Z, Li X, Hu Z, Yang Y, Yang Z, Li S, Zhou Y, Ma J, Li H, Liu X, *et al*: Linc00996 is a favorable prognostic factor in LUAD: Results from bioinformatics analysis and experimental validation. Front Genet 13: 932973, 2022.
39. Ge H, Yan Y, Wu D, Huang Y and Tian F: Potential role of LINC00996 in colorectal cancer: a study based on data mining and bioinformatics. Onco Targets Ther 11: 4845-4855, 2018.
40. Berek JS, Renz M, Kehoe S, Kumar L and Friedlander M: Cancer of the ovary, fallopian tube, and peritoneum: 2021 update. Int J Gynaecol Obstet 155 (Suppl): 61-85, 2021.
41. Kawase K, Kawashima S, Nagasaki J, Inozume T, Tanji E, Kawazu M, Hanazawa T and Togashi Y: High expression of MHC class I overcomes cancer immunotherapy resistance due to IFNγ signaling pathway defects. Cancer Immunol Res 11: 895-908, 2023.
42. Hiltner T, Szörenyi N, Kohlruss M, Hapfelmeier A, Herz AL, Slotta-Huspenina J, Jesinghaus M, Novotny A, Lange S, Ott K, *et al*: Significant tumor regression after neoadjuvant chemotherapy in gastric cancer, but poor survival of the patient? Role of MHC class I alterations. Cancers (Basel) 15: 771, 2023.
43. Colbert JD, Cruz FM, Baer CE and Rock KL: Tetraspanin-5-mediated MHC class I clustering is required for optimal CD8 T cell activation. Proc Natl Acad Sci USA 119: e2122188119, 2022.
44. Luda KM, Longo J, Kitchen-Goosen SM, Duimstra LR, Ma EH, Watson MJ, Oswald BM, Fu Z, Madaj Z, Kupai A, *et al*: Ketolysis drives CD8+ T cell effector function through effects on histone acetylation. Immunity 56: 2021-2035.e8, 2023.
45. Stanifer ML, Guo C, Doldan P and Boulant S: Importance of type I and III interferons at respiratory and intestinal barrier surfaces. Front Immunol 11: 608645, 2020.
46. Chen L, Min J and Wang F: Copper homeostasis and cuproptosis in health and disease. Signal Transduct Target Ther 7: 378, 2022.
47. O'Day S, Gonzalez R, Lawson D, Weber R, Hutchins L, Anderson C, Haddad J, Kong S, Williams A and Jacobson E: Phase II, randomized, controlled, double-blinded trial of weekly elesclomol plus paclitaxel versus paclitaxel alone for stage IV metastatic melanoma. J Clin Oncol 27: 5452-5458, 2009.
48. Guo CJ, Ma XK, Xing YH, Zheng CC, Xu YF, Shan L, Zhang J, Wang S, Wang Y, Carmichael GG, *et al*: Distinct processing of lncRNAs contributes to non-conserved functions in stem cells. Cell 181: 621-636.e22, 2020.
49. Wang Q, Li G, Ma X, Liu L, Liu J, Yin Y, Li H, Chen Y, Zhang X, Zhang L, *et al*: LncRNA TINCR impairs the efficacy of immunotherapy against breast cancer by recruiting DNMT1 and downregulating MiR-199a-5p via the STAT1-TINCR-USP20-PD-L1 axis. Cell Death Dis 14: 76, 2023.
50. Priyanka P, Sharma M, Das S and Saxena S: The lncRNA HMS recruits RNA-binding protein HuR to stabilize the 3'-UTR of HOXC10 mRNA. J Biol Chem 297: 100997, 2021.
51. Latorre E, Carelli S, Raimondi I, D'Agostino V, Castiglioni I, Zucal C, Moro G, Luciani A, Ghilardi G, Monti E, *et al*: The ribonucleic complex HuR-MALAT1 represses CD133 expression and suppresses epithelial-mesenchymal transition in breast cancer. Cancer Res 76: 2626-2636, 2016.
52. Brennan CM and Steitz JA: HuR and mRNA stability. Cell Mol Life Sci 58: 266-277, 2001.
53. Fu XD: RNA editing: New roles in feedback and feedforward control. Cell Res 33: 495-496, 2023.
54. Hildebrandt RP, Moss KR, Janusz-Kaminska A, Knudson LA, Denes LT, Saxena T, Boggupalli DP, Li Z, Lin K, Bassell GJ, *et al*: Muscleblind-like proteins use modular domains to localize RNAs by riding kinesins and docking to membranes. Nat Commun 14: 3427, 2023.
55. González ÀL, Fernández-Remacha D, Borrell JI, Teixidó J and Estrada-Tejedor R: Cognate RNA-binding modes by the alternative-splicing regulator MBNL1 inferred from molecular dynamics. Int J Mol Sci 23: 16147, 2022.
56. Liu Y, Wei W, Wang Y, Wan C, Bai Y, Sun X, Ma J and Zheng F: TNF-α/calreticulin dual signaling induced NLRP3 inflammasome activation associated with HuR nucleocytoplasmic shuttling in rheumatoid arthritis. Inflamm Res 68: 597-611, 2019.
57. Jeyabal P, Thandavarayan RA, Joladarashi D, Suresh Babu S, Krishnamurthy S, Bhimaraj A, Youker KA, Kishore R and Krishnamurthy P: MicroRNA-9 inhibits hyperglycemia-induced pyroptosis in human ventricular cardiomyocytes by targeting ELAVL1. Biochem Biophys Res Commun 471: 423-429, 2016.